ELSEVIER

Chemical Geology 152 (1998) 257–271

CHEMICAL GEOLOGY
INCLUDING
ISOTOPE GEOSCIENCE

The thermal and cementation histories of a sandstone petroleum reservoir, Elk Hills, California
Part 2: in situ oxygen and carbon isotopic results

Keith I. Mahon *, T. Mark Harrison, Kevin D. McKeegan

Department of Earth and Space Sciences and Institute of Geophysics and Planetary Physics, University of California, Los Angeles, CA 90095-1567, USA

Received 8 August 1997; accepted 18 June 1998

Abstract

Liquid hydrocarbon accumulations within the Elk Hills and North Coles Levee oil fields, southern San Joaquin basin, are largely isolated within calcite-cemented reservoirs comprised of late Miocene Stevens sandstone. We undertook ion microprobe carbon and oxygen isotope ratio measurements on calcite cements to assess both the source of the carbon and the temperature of cementation. By combining thermal history results from $^{40}Ar/^{39}Ar$ analyses (reported in the companion study) with calculated cementation temperatures based on our oxygen isotope measurements, a model cementation history is derived which indicates that carbonate precipitation occurred primarily between 4 and 6.5 Ma. Conventional oxygen isotopic measurements yield a more restricted range of isotopic compositions reflecting the averaging properties of that method. The associated carbon isotopic measurements suggest that most of the early cements were derived from a marine carbonate source or a mixture of marine carbonate and lighter carbon from maturing hydrocarbons. Carbonates precipitated most recently (and thus at the highest temperatures) contain light carbon, interpreted to result from thermal decomposition of kerogen in the interbedded shales. Based on the light carbon values ($< -10‰_{PDB}$) and low range of temperatures over which the bulk of the cement formed, the maturation of petroleum in the interbedded shales likely postdates cementation.

Keywords: Elk Hills field; Kern County, California; Ion probe; Stable isotopes; Thermal history, diagenesis

1. Introduction

Understanding the timing of diagenetic changes that occur in sedimentary basins is of potential benefit in exploiting both the geodynamic and economic importance of these features. Determining the time-dependent storage capacity of partially cemented petroleum reservoirs may help in constraining the physical character of a reservoir and perhaps in developing strategies for enhanced oil recovery. The evolution of porosity and permeability in sandstone petroleum reservoirs reflects a variety of diagenetic processes, including compaction, pressure solution, dissolution, and cementation (Houseknecht, 1987;

---

* Corresponding author. Exxon Production Research Company, P.O 2189, Houston, TX 77252-2189, USA. Fax: +1 713 431 7279.

PII: S0009-2541(98)00116-8

Pate, 1989; Ehrenberg, 1989; Wood and Boles, 1991; Taylor and Soule, 1993; Robinson et al., 1993; Feldman et al., 1993). However, porosity and permeability are only weakly correlated with depth and can vary considerably within stratigraphic units of the reservoir rocks (Taylor and Soule, 1993). Variations in permeability along bedding planes due to the cementing action of migrating water, mainly due to heterogeneities in deposition and the dynamics of diagenesis, are difficult to assess accurately (Craft and Hawkins, 1991). Knowledge of the isotopic variability of diagenetic cements could provide insight into the scale of pore fluid migration as well as provide estimates of the temperature and pore fluid composition at the time of cement formation.

Wood and Boles (1991) developed an interpretive model for the cementation history of the Stevens sandstone at North Coles Levee (NCL), southern San Joaquin Basin, based on stable isotope fractionations inferred from measurements of bulk carbonate cements (Boles and Ramseyer, 1987; Schultz et al., 1989). Assuming a model evolution for the pore fluid at NCL, they calculated cementation temperatures using known water–mineral fractionation thermometers (e.g., Friedman and O’Neil, 1977). Coupled with a thermal history inferred from a depositional model, they then estimated the approximate timing of cementation.

Wood and Boles (1991) concluded that cementation of the Stevens sandstone at NCL occurred in discrete stages; an early cementation of dolomitic concretions was followed by a mixed phase involving calcite cementation together with a component derived from thermal maturation of deeply buried organic matter, and finally by an episode of calcite cementation from a marine source. They interpreted this sequence of cementation events to reflect early biologic concretions followed by discrete episodes of

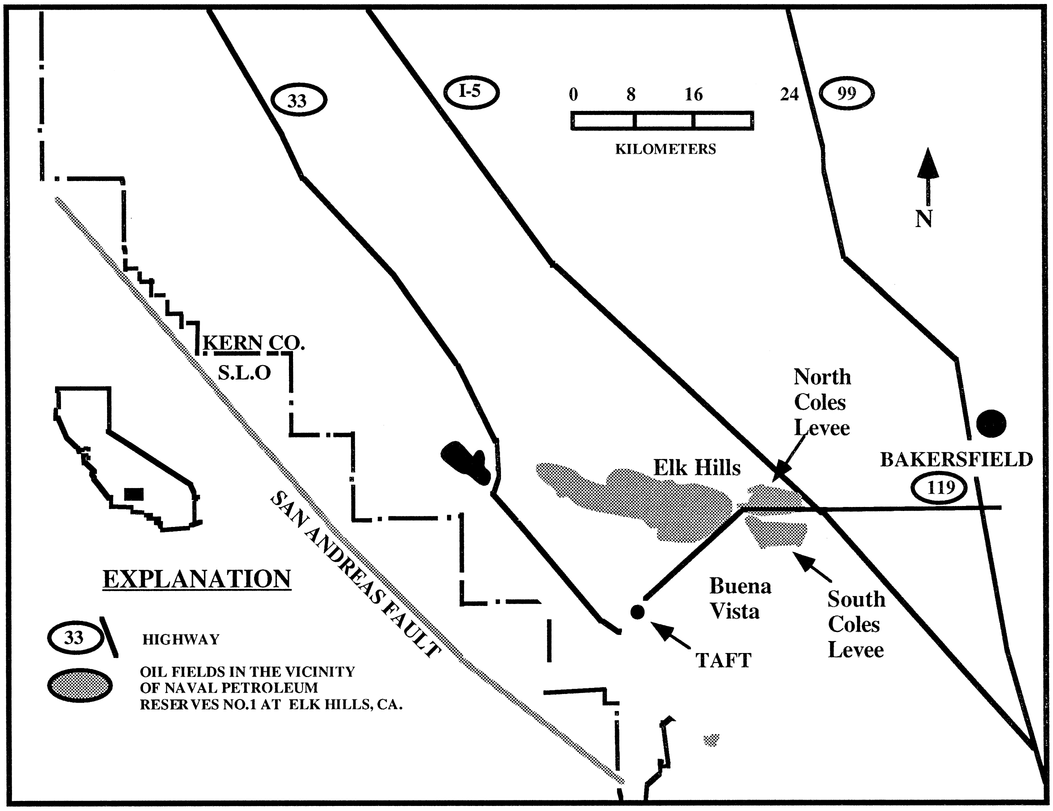

Fig. 1. Map showing the locations of the Elk Hills and Coles Levee oil fields, southern San Joaquin basin, CA. Modified from Reid (1990).

calcite cementation that originate from large volumes of pore fluids that entered a region of the reservoir along faults and fractures during major seismic events. Because this model was based on analyses of milligram quantities of carbonate cement (Boles and Ramseyer, 1987), which are necessarily mixtures of multiple generations of cementation developed at the 1 to 100 μm scale, these measurements provide an average value of isotopically heterogeneous material. Resolving multiple generations of cementation at the ~ 10-μm scale by in situ isotopic analysis would both directly test the Wood–Boles hypothesis and provide a high spatial resolution record of cement growth conditions.

We have used an ion microprobe to perform in situ carbon and oxygen isotopic analyses of multiple generations of calcite cements from petrographically characterized core samples from the Stevens sands (Monterey formation) at both Elk Hills and NCL from the southern San Joaquin basin (Fig. 1). Because this region includes the deepest well in California (thus providing access to a wide spectrum of temperatures), and since it is directly adjacent to the NCL oil field with which it shares numerous stratigraphic features, it constitutes an appropriate environment in which to test the Wood and Boles (1991) diagenetic model. In a companion paper, we describe the geology of the Naval Petroleum Reserve Number 1 (NPR-1) at Elk Hills and develop a model of the thermal evolution of the basin derived from ^{40}Ar/^{39}Ar thermochronometry (Mahon et al., 1998). Here we combine our new isotopic measurements with that thermal history to assess the feasibility of determining the evolution of cementation within this portion of the basin.

2. Geological background

The Elk Hills and Coles Levee oil fields are located in the southern San Joaquin basin, CA (Fig. 1). The geological setting is described in detail in the companion paper (Mahon et al., 1998). Briefly, the San Joaquin basin formed in the late Cretaceous as a fore-arc basin and continued as a major depocenter following the development of the San Andreas transform system. Convergence of the Pacific and North American plates resulted in the development of en echelon fault-bend folds along the western edge of San Joaquin basin (Davis and Lagoe, 1988; Fishburn, 1990; Nilsen and Sylvester, 1995). An amalgamation of sands and organic-rich shales, derived from denudation of adjacent batholiths of largely Cretaceous age, was deposited in the southern San Joaquin basin (Graham and Williams, 1985; Bent, 1988). Turbidites were deposited within the Monterey formation during the mid to late Miocene in much of the southern San Joaquin basin. At Elk Hills and NCL, such turbidite sands, referred to as the Stevens zone (Reid, 1990), were deposited during the upper Mohnian (10 − 6 Ma; Calloway, 1990).

3. Analytical methods

3.1. Sampling strategy

During the diagenesis of clastic sedimentary rocks, unstable precursor phases undergo incongruent dissolution as they react with pore fluids. These locally-derived dissolved solids are typically re-precipitated as cements. Additional cements may be precipitated from externally-derived fluids. Stable isotope compositions of these cements potentially identify source regions and permit estimation of the pore fluid composition and/or temperature at the time of cementation. The typical cement in the Stevens sandstone at Elk Hills and NCL is carbonate with lesser amounts of quartz and clays (Tieh et al., 1986; Reid, 1990; Wood and Boles, 1991). In addition to intergranular cements, cross-cutting calcite veins are also present in the NCL and Elk Hills samples.

We obtained a suite of cores from the upper Main Body B at Elk Hills (well 352X-3G) and the Main Western at NCL (well 488-29), both within the Stevens oil zone of the Monterey formation. Sample descriptions are given in Appendix A. Cores recovered from an adjacent borehole, 934-29R, the deepest well within the Naval Petroleum Reserve 1 (NPR-1) at Elk Hills (Fishburn, 1990; McJanet, 1993), yielded detrital K-feldspar separates that were analyzed by ^{40}Ar/^{39}Ar thermochronometry (Mahon et al., 1998). These data constrain a thermal model of basin evolution that predicts the thermal history of horizons spatially equivalent to the Stevens sands at NCL.

Polished thin sections of the samples were obtained for petrographic and back-scattered electron imaging in order to document the textural relationships between multiple generations of cement. Conventional carbon and oxygen isotope ratio measurements of calcite cements were made from the same drill cores by differential acid dissolution of the sandstones to characterize their average isotopic compositions. We then analyzed the corresponding polished sections using the ion microprobe to determine oxygen and carbon isotopic variations at the 10-μm scale. Although volumetrically insignificant in our samples from Elk Hills and NCL, quartz cements occur in many sandstone reservoirs. Ion microprobe oxygen isotopic measurements of quartz cements have been shown to be useful in establishing relative timing of diagenetic processes in such environments (e.g., Hervig et al., 1995; Graham and Valley, 1996).

3.2. Conventional stable isotope analysis

Calcite-bearing samples were crushed into a fine powder in a ceramic mortar and pestle. Approximately 10 mg of the calcite standard was reacted with H_3PO_4, and the CO_2 gas evolved was analyzed mass spectrometrically. Because the cemented sandstones investigated in this study contain between 15 and 35% calcite, ~100 mg of the crushed sample was reacted to ensure sufficient quantities of CO_2 for analysis. Methods for the isotopic analysis of bulk carbonate samples followed that of Craig (1957); precision and accuracy are estimated to be 0.1–0.2‰ for $\delta^{18}O$ and $\delta^{13}C$.

3.3. Ion microprobe stable isotopic analysis

Ion microprobe measurements permit in situ isotopic analysis with high spatial resolution [see the work of Ireland (1995) for a review]. Our measurements were made with the UCLA CAMECA ims 1270 ion microprobe using a Cs^+ primary ion beam (de Chambost et al., 1991). Negative secondary ions were analyzed and a normal incidence electron flood gun was used to neutralize positive charge buildup on the insulating samples (Slodzian et al., 1987).

Analysis of oxygen and carbon isotopic ratios were performed by magnetic peak-switching. Measurements were made at a mass resolving power $(M/\Delta M)$ of ~4000, sufficient to eliminate all isobaric interferences (e.g., $^{13}C^-$ vs. $^{12}CH^-$), by sputtering with a ~0.5 nA Cs^+ primary beam (impact energy ~20 keV) which was defocused to produce a roughly circular, flat-bottomed crater of ~10 to 20 μm diameter. Some (earlier) analyses were obtained by pulse-counting with an electron multiplier (EM) only, while later oxygen isotope analyses used a Faraday cup (FC) to measure the intense $^{16}O^-$ signal and the EM for the $^{18}O^-$ peak. This method has the advantage of permitting a large increase in the instrument transmission (factor of ~50), and the increased intensity for $^{18}O^-$ on the EM results in reduced analysis time (~5–10 min) to obtain the same precision as those analyses where the intensity (i.e., transmission) is restricted to avoid saturation of the $^{16}O^-$ signal on the EM. Analyses were corrected for deadtime (EM) and background (FC). During the course of these experiments, the measured EM deadtime varied between 16 and 34 ns, depending on multiplier age, but could be determined with better than 10% accuracy. Especially for the EM only experiments, care was taken to keep count rates on both standards and unknowns at similar levels (~10^6/s for $^{16}O^-$) to minimize the effect that uncertainty in the EM deadtime may have on the results. The mixed detector measurements are comparatively insensitive to errors in the deadtime correction because the count rates for $^{18}O^-$ never exceeded ~2×10^5/s even for the most intense ion beams.

The EM only measurements typically comprised 100 cycles of counting the major isotope (^{12}C or ^{16}O) for 2 s and the minor isotope (^{13}C or ^{18}O) for 10 s. With these conditions, an internal precision of < 1‰ (1 standard error of the mean) was routinely obtained for both $\delta^{18}O$ and $\delta^{13}C$ for analyses lasting ~20 min. The oxygen isotope measurements that utilized mixed detectors integrated for 3 s on $^{16}O^-$ (FC) and 5 s on the EM for $^{18}O^-$. Typically, 20 to 40 cycles were measured which resulted in ~0.5‰ internal precision. The external reproducibility (i.e., between analyses on different spots of standards and unknowns) in this measurement method is critically dependent on the stability of the EM gain relative to the FC. Provided that count rates on the EM are kept low (< few times 10^5/s), long-term drift of mea-

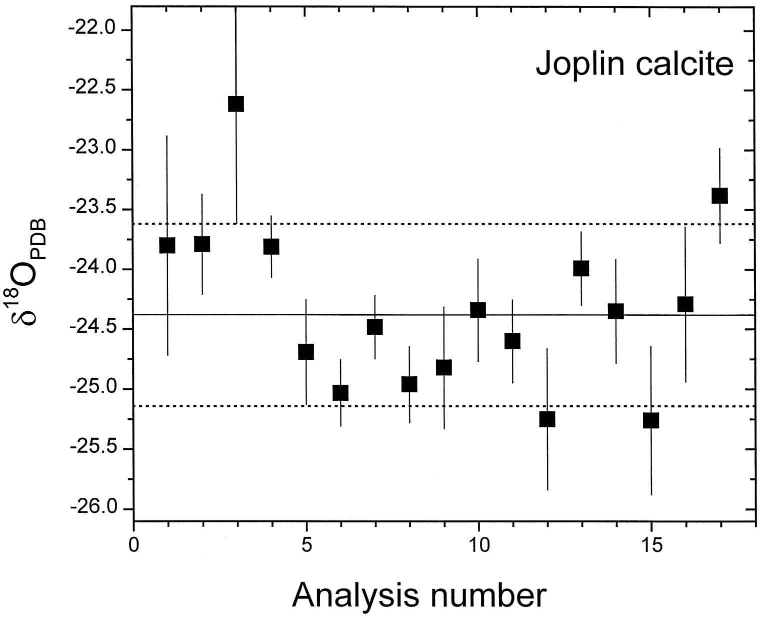

Fig. 2. External reproducibility of oxygen isotope analyses of the Joplin calcite standard during an analytical session where a mixed detector mode (Faraday cup and electron multiplier) was employed. Shown are mass-fractionation corrected $\delta^{18}O$ values with 1σ error bars for 17 individual analysis spots. Although there is some small additional scatter beyond the internal measurement errors, there is no apparent drift of isotopic ratios with time that would indicate a significant change in relative efficiency between the two detectors. A good estimate of the overall spot-to-spot reproducibility of the measurement technique is given by the standard deviation of the entire population (dashed lines) which in this case is ~ 0.8‰.

sured isotope ratios during an analytical session which could be ascribed to a decrease of EM gain with time are generally not resolvable. For example, Fig. 2 shows a sequence of 17 oxygen isotopic measurements of different spots of the Joplin calcite standard (see below) made over a 24-h analysis session. As expected, the data show some additional scatter beyond the internal precision (reduced $\chi^2 = 2.0$), however there is no systematic trend and the data are consistent with a single population with a standard deviation equal to 0.76‰. This value may be taken as representative of the overall point-to-point reproducibility of the method, while the uncertainty in the mean composition for repeated analysis of a homogeneous material is on the order of 0.2‰ (1 standard error of the mean).

Instrumental mass fractionation was corrected for by analyses of standard materials interspersed with those of the unknowns. Since only near end-member calcite cements were measured (Appendix A), complications due to matrix effects do not arise (e.g., Valley et al., 1997). Two calcite crystals were isotopically characterized for use as ion microprobe standards: ‘Optical calcite’ (MS1212G Mexico), and ‘Joplin calcite’ from Joplin, Missouri, Conventional acid-dissolution measurements of aliquots of optical calcite yielded $\delta^{18}O_{PDB} = -13.55 \pm 0.15$‰ and $\delta^{13}C_{PDB} = -10.98 \pm 0.10$‰ and bulk Joplin calcite yielded $\delta^{18}O_{PDB} = -24.38 \pm 0.12$‰ and $\delta^{13}C_{PDB} = -5.58 \pm 0.10$‰. The accuracy of the mass fractionation-corrected SIMS measurement was tested by treating the Optical calcite as a primary standard and

Table 1
Comparison between conventionally determined and ion microprobe analyses of Joplin calcite standard

	N	Conventional	Ion microprobe	reduced χ^2
$\delta^{18}O_{PDB}$	11	-24.38 ± 0.12‰	-24.3 ± 0.4‰	1.4
$\delta^{13}C_{PDB}$	13	-5.58 ± 0.10‰	-5.7 ± 0.3‰	2.3

N represents the number of ion microprobe analyses; errors quoted are $1\sigma_{mean}$.

the Joplin sample as an ‘unknown’. Ion microprobe measurements (Table 1) yield oxygen and carbon isotopic values for Joplin calcite of $\delta^{18}O_{PDB} = -24.3 \pm 0.4‰$ and $\delta^{13}C_{PDB} = -5.7 \pm 0.3‰$ which agree well with the gas mass spectrometry measurements.

4. Results

4.1. Conventional stable isotope analysis

The results of acid dissolution carbon and oxygen isotopic measurements of the calcite cemented samples from the Stevens zone at Elk Hills and the calcite–dolomite cemented samples from NCL are given in Table 2 (listed as ‘Bulk’ values). The $\delta^{18}O_{PDB}$ values vary from −6.7 to −4.3‰ and $\delta^{13}C_{PDB}$ values ranged from −9.2 to +2.1‰. This represents considerably lower heterogeneity than that reported by Wood and Boles (1991) who found variations of ~10‰ in $\delta^{18}O$ and ~20‰ for $\delta^{13}C$ from bulk analyses of carbonate cements at NCL. This may be due in part to the much broader depth range assessed by Wood and Boles at NCL (2609 to 2768 m) whereas the analyses from this study of Elk Hills is restricted to a 35-m interval (2182 to 2217 m).

4.2. Ion microprobe stable isotopic analysis

Sandstone samples from Elk Hills and NCL were mounted in 1 in. diameter epoxy disks together with standard materials and analyzed for oxygen and carbon isotopic compositions of the calcite cements. Initial analyses were undertaken using petrographic thin sections polished to a thickness of ~60 μm. However, the epoxy impregnation led to contamination preferentially along grain boundaries and cracks that appears to have compromised some carbon isotopic measurements. We attempted to correct for this contamination by monitoring $^{12}CH^-/^{12}C^-$, which is 10^3 times greater in epoxy than in calcite, but subsequently avoided this problem by using only non-epoxy-impregnated, polished, ~1-mm thick sections.

Oxygen isotopic analysis of EH95 was complicated by the presence of diagenetic or detrital quartz within the carbonate cements. This appeared to be a significant problem with NCL-29-A-1, where a narrow (20 μm) carbonate vein cut through a detrital

Table 2
Ion microprobe carbon and oxygen isotopic results for Elk Hills and North Coles Levee samples

	$\delta^{13}C_{PDB}$	$\delta^{18}O_{PDB}$
EH-3G-B-6a (B6a)		
Bulk	+2.1 ± 0.1‰	−5.8 ± 0.2‰
Cement-EH95 (1)	−0.3 ± 0.5‰	−6.3 ± 1.3‰
EH-3G-B-7a (B7a)		
Bulk	−4.3 ± 0.1‰	−5.6 ± 0.2‰
Cement-EH95 (C13)	−9.0 ± 0.5‰	
Vein-EH95 (C10v)	+0.1 ± 0.5‰	
Vein-EH95 (C11v)	+0.4 ± 0.4‰	
Cement EH96a (7 and 8)	−7.3 ± 0.6‰	
Cement-EH95 (1 and 2)		−3.0 ± 0.7‰
Vein-EH95 (8v, 9v, and 10v)		−4.0 ± 0.4‰
Cement EH96a (9)		−8.8 ± 0.4‰
Cement EH96a (10 and 11)		−6.8 ± 0.3‰
EH-3G-B-7c (B7c)		
Bulk	−5.1 ± 0.1‰	−6.2 ± 0.2‰
Cement EH96a (1, 3, and 5)	−13.2 ± 0.6‰	
Cement EH96a (2 and 4)	−9.6 ± 0.4‰	
Cement EH96a (6 and 7)		−11.6 ± 0.4‰
Cement EH96a (8)		−8.8 ± 0.4‰
EH-3G-B-7e (B7e)		
Bulk	−6.4 ± 0.1‰	−6.7 ± 0.2‰
Cement EH96a (1, 2, 3, and 4)	−10.2 ± 0.6‰	
Cement EH96a (5 and 7)		−9.8 ± 0.4‰
Cement EH96a (6)		−5.0 ± 0.6‰
EH-3G-B-8 (B8)		
Bulk	+1.9 ± 0.1‰	−4.3 ± 0.2‰
Cement-EH95 (C1)	−5.8 ± 0.5‰	
Cement-EH95 (C2)	−10.0 ± 0.5‰	
Cement EH96a (4)	−0.7 ± 0.8‰	
Cc xtal EH96a (5)	+6.2 ± 0.7‰	
Cement-EH95 (1)		−4.5 ± 0.9‰
Cement − EH95 (2)		−7.5 ± 0.9‰
Cement EH96a (17 and 18)		−1.2 ± 0.3‰
Cement EH96a (19 and 22)		−5.4 ± 0.4‰
Cc xtal EH96a (20 and 21)		−3.0 ± 0.4‰
NCL-29-A-1		
Bulk	−9.2 ± 0.1‰	−6.6 ± 0.2‰
Cement-EH95 (C3)	−6.8 ± 0.4‰	
Cement-EH95 (C4)	−9.3 ± 0.4‰	
Vein-EH95 (C1v and C6v)	−8.9 ± 0.4‰	
Cement-EH95 (1, 3, and 4)		−11.8 ± 0.8‰
Vein-EH95 (1v, 4v, and 5v)		−10.1 ± 0.5‰
Vein-EH95 (2v and 3v)		−13.9 ± 0.5‰

quartz crystal. We monitored the $^{28}Si^{-}$ intensity during the analysis to assess the magnitude of the possible contribution of quartz to the total oxygen isotope signal. The maximum correction required was < 0.1‰ which is negligible relative to overall uncertainties. Table 2 contains carbon and oxygen isotopic results that we consider to be accurate (i.e., free from significant epoxy, quartz, or other contaminants). The oxygen isotopes vary from -13.9 to -1.2 $\delta^{18}O_{PDB}$ and carbon from -13.2 to $+6.2$ $\delta^{13}C_{PDB}$. In some cases, spatially clustered analyses yielded results that were statistically indistinguishable and were aggregated into a single datum for the purposes of thermometry.

5. Discussion

5.1. Isotopic heterogeneity, paleotemperature, and carbon sources

As expected, the ion microprobe carbon and oxygen isotope ratio measurements of the cements show greater variation compared to the conventional stable isotope analyses. The complexity due to multiple generations of calcite cementation in the Steven's sands is well illustrated by the results from samples B7a and B8. Whereas the bulk $\delta^{18}O_{PDB}$ of EH-3G-B-7a is -5.6‰, the in situ results (Fig. 3) range from -8.8 to -3.0‰. Similarly, the bulk $\delta^{13}C_{PDB}$ of -4.3‰ is intermediate to the range of in situ

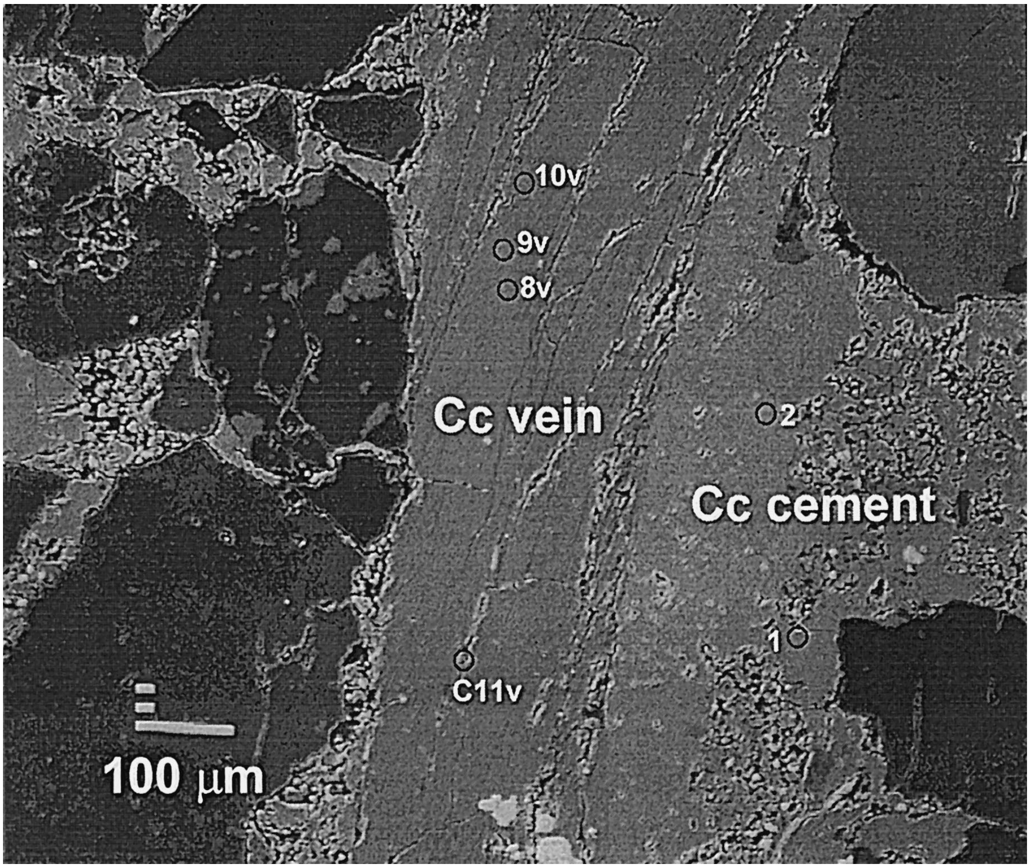

Fig. 3. Backscattered electron image of sample EH-3G-B-7a (B7a) (mount EH95) from Elk Hills showing the location of the calcite vein and some spot analyses.

results of −9.0 to +0.4‰. For EH-3G-B-8 (Fig. 4), the bulk $\delta^{18}O_{PDB}$ of −4.3‰ is bounded by the in situ values of −7.5 to −1.2‰ and the bulk $\delta^{13}C_{PDB}$ + 1.9‰ is between the in situ results, which however range from −10.0 to +6.2‰. The advantage of in situ analysis in correlating isotopic information with specific textural relationships is also exemplified by sample B7a. In this section, calcite cements are cross-cut by a clearly later generation calcite vein (Fig. 3). The isotopic compositions of these two calcites differ by 9‰ in $\delta^{13}C$ but are similar in $\delta^{18}O$.

The isotopic composition of oxygen in carbonate cements can be used to estimate the temperature of carbonate precipitation. However, this is predicated on knowledge of the isotope composition of the pore fluid in equilibrium with the cement during formation. Although the isotopic composition of ocean water during the Miocene was constant to ±1‰ (Woodruff et al., 1981), water in the partially closed San Joaquin basin may have varied during deposition of the Stevens sands (Graham and Williams, 1985). Several workers have successfully constrained the possible variation in oxygen isotope composition of pore fluids during burial and recrystallization of marine carbonates (Killingley, 1983; Richter and DePaolo, 1987; Schrag et al., 1992, 1995) by using the measured compositions of residual solids and modern pore fluids. At NCL, Wood and Boles (1991) assumed a linear increase in $\delta^{18}O_{SMOW}$ of pore fluids over time from 0‰ to +4‰, the present measured value of brines from the Stevens sands at NCL. Unfortunately, the brines from the non-produc-

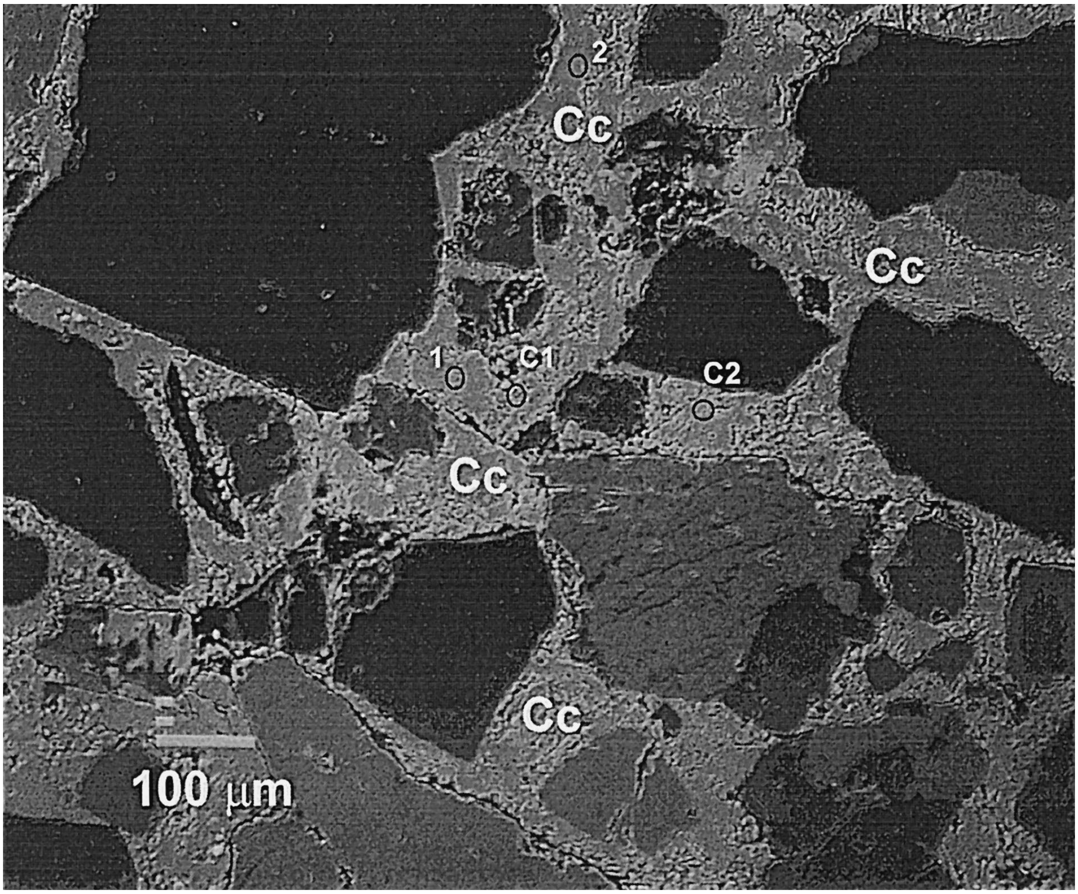

Fig. 4. Backscattered electron image of sample EH-3G-B-8 (B8) (mount EH95) from Elk Hills showing the location of some spot analyses.

ing, exploratory wells at Elk Hills are contaminated by drilling products precluding a similar approach here.

We consider two models for the isotopic composition of the pore fluid during cementation. Model I assumes a constant value equivalent to late Miocene seawater (i.e., $\delta^{18}O_{SMOW} = 0‰$). This model would be particularly applicable to the case in which cementation of the 7 Ma Stevens sands occurs within several million years of deposition prior to uplift of the submarine basin and therefore not subject to meteoric influence. In this model, clay mineral reactions capable of enriching pore fluids in ^{18}O are neglected since reaction rates would be enhanced by high temperatures that have only recently been attained in the Stevens sands. Even in the case where significant water–rock interactions have occurred, the calculated temperatures could be viewed as minimum values.

Model II uses the Wood and Boles (1991) assumption of a linear change in time from the late Miocene seawater value (0‰) to the present observed value (+4‰) at NCL. As the typical range of $\delta^{18}O_{SMOW}$ values in brines of the southern San Joaquin basin, including Elk Hills, is between 0 and +4‰ (Kharaka et al., 1973; Wood and Boles, 1991; T. Torgerson, pers. comm., 1997), this approach would seem to better reflect the changing pore fluid composition.

The temperature of carbonate precipitation for either model is calculated from the relationship:

$$T\,(°C) = \left(2.78 \times 10^6 / \left(\delta^{18}O_{sample} - \delta^{18}O_{water} + 2.89\right)\right)^{1/2} - 273 \qquad (1)$$

where the isotope compositions are relative to SMOW, fractionation parameters are for calcite–water from Friedman and O'Neil (1977), and the standard error for model I is given by:

$$\sigma_{T[I]} = \left(1/2(2.78 \times 10^6)^{1/2} / \left(\delta^{18}O_{sample} - \delta^{18}O_{water} + 2.89\right)^{3/2}\right) \sigma\,\delta^{18}O_{sample}$$

The standard error for Model II is:

$$\sigma_{T[II]} = \sqrt{2}\,\sigma_{T[I]}$$

Model I temperatures are calculated in a straightforward manner. In Model II however, the linear time dependence assumed by Wood and Boles (1991) for $\delta^{18}O_{water}$ implies that this variable is also implicitly a function of temperature. We have constrained the relationship between temperature and $\delta^{18}O_{water}$ within the Stevens sand by extrapolating the $^{40}Ar/^{39}Ar$ K-feldspar thermal history results described in the work of Mahon et al. (1998) from deeper levels to this horizon. Specifically we equated the late Miocene sea water value ($0‰_{SMOW}$) to a temperature of 20°C and the present observed value ($+4‰_{SMOW}$) to 95°C and interpolated $\delta^{18}O_{water}$ at different temperatures by assuming a linear increase with time (Table 3). Model II temperatures were obtained by the recursive formula given in Eq. (1). Trial values of $\delta^{18}O_{water}$ were input to obtain a temperature. The value of $\delta^{18}O_{water}$ corresponding to this temperature was then input to obtain a new temperature. Eq. (1) converges to within 1°C of the final value within a few iterations. For example, B7a, which has a bulk $\delta^{18}O_{PDB} = -5.60 \pm 0.15‰$, converges to a calculated temperature of 48 ± 2°C after four iterations with a fluid composition equal to $\delta^{18}O_{SMOW} = 1.1‰$. Assuming a constant water composition of $0‰_{SMOW}$, the same sample yields a temperature of 42 ± 1°C. The oxygen isotopic data listed in Table 2 were used to calculate temperatures according to both models, which are tabulated in Table 4.

Spots 1, 3, and 4 on section NCL-29-A-1 yield model II temperatures well above the present temperature of 95°C [see the work of Wood and Boles

Table 3
Estimated temperature history of the Stevens sands, Elk Hills [from the work of Mahon et al. (1998)]

Time (Ma)	Depth (m)	Temperature (°C)	Model II fluid $\delta^{18}O_{SMOW}$ (‰)
7	5	20	0.0
6	305	33	0.6
5	805	51	1.1
4	1305	68	1.7
3	1655	80	2.3
2	1855	87	2.9
1	1955	92	3.4
0	2005	95	4.0

Table 4
Calculated cement formation temperatures

	Model I (°C)	Model II (°C)
EH-3G-B-6a (B6a)		
Bulk Oxygen	43 ± 1	50 ± 2
Cement-EH95 (1)	46 ± 8	55 ± 12
EH-3G-B-7a (B7a)		
Bulk Oxygen	42 ± 1	48 ± 2
Cement-EH95 (1,2)	28 ± 3	28 ± 4
Vein-EH95 (8v, 9v, 10v)	33 ± 2	35 ± 3
Cement EH96a (9)	62 ± 3	84 ± 5
Cement EH96a (10, 11)	49 ± 2	60 ± 3
EH-3G-B-7c (B7c)		
Bulk Oxygen	45 ± 1	54 ± 2
Cement EH96a (6, 7)	84 ± 3	144 ± 8
Cement EH96a (8)	62 ± 3	84 ± 5
EH-3G-B-7e (B7e)		
Bulk Oxygen	48 ± 1	59 ± 2
Cement EH96a (5, 7)	69 ± 3	99 ± 5
Cement EH96a (6)	38 ± 3	43 ± 5
EH-3G-B-8 (B8)		
Bulk Oxygen	35 ± 1	38 ± 2
Cement-EH95 (1)	36 ± 5	39 ± 7
Cement-EH95 (2)	53 ± 6	67 ± 9
Cement EH96a (17, 18)	19 ± 1	17 ± 2
Cement EH96a (19, 22)	41 ± 2	47 ± 3
Cc xtal EH96a (20, 21)	28 ± 2	28 ± 3
NCL-29-A-1		
Bulk Oxygen	48 ± 1	58 ± 2
Cement-EH95 (1, 3, 4)	85 ± 7	152 ± 16
Vein-EH95 (1v, 4v, 5v)	72 ± 4	105 ± 7
Vein-EH95 (2v, 3v)	105 ± 5	–

(1991)]. On the other hand, model I results suggest that the carbonate vein may have been filled quite recently, based on the temperature estimates from spots 2v and 3v (see Table 4). Perhaps the enrichment of pore fluids in ^{18}O is a more recent phenomena at NCL and postdated the cementation of the Stevens sands. An assumed pore fluid composition of $0‰_{\mathrm{SMOW}}$ (Model I) for the Elk Hills samples results in a wide range of precipitation temperatures for the spots analyzed (19 to 84°C), with the majority below 50°C. Model I temperatures all fall within or near the bounds set by the temperature at deposition (~ 20°C) and the present day value at the depth corresponding to the Stevens sands (~ 95°C). Furthermore, results from zoned cements and cross-cutting relationships are internally consistent. For clarity in the subsequent discussion, we refer only to model I temperatures.

Several inferences can be drawn regarding the source and temperature of the fluids in equilibrium with the precipitating carbonate for the most analyzed samples (B7a and B8) that are generally independent of the chosen model. The calculated 'bulk' paleotemperature for sample B7a (assuming $0‰_{\mathrm{SMOW}}$) is 42°C. However, the in situ measurements indicate an early cementation event at 28°C (Table 4) from a fluid derived in part from a methanogenic source (i.e., sample EH95 C13 has $\delta^{13}\mathrm{C}_{\mathrm{PDB}} = -9.0‰$; Table 2) that is cut by a vein of marine carbonate origin with a calculated temperature of 33°C (i.e., C10v, C11v with $\delta^{13}\mathrm{C}_{\mathrm{PDB}} \sim 0‰$; Table 2). Later generations of cementation yield paleotemperatures of 49°C and 62°C (EH96a) with the former resulting from a fluid of mixed marine and methanogenic sources. These results are both internally consistent and appear to yield a sensible thermostratigraphy. This behavior is also observed in other samples. For example, the lowest calculated temperature from a B8 cement is 19°C (Table 4) (note that no in situ carbon measurements were obtained on this portion of the section). Later, a subhedral crystal of calcite formed at ~ 28°C from a fluid strongly enriched in ^{13}C, perhaps due to bacterial action. This is followed by cementation events identified at 36°C from a fluid from a mixed source ($\delta^{13}\mathrm{C}_{\mathrm{PDB}} = -5.8‰$). At ~ 41°C, another cement precipitates from a marine carbonate source ($\delta^{13}\mathrm{C}_{\mathrm{PDB}} = -0.7‰$). The last recorded cementation event occurs at a model temperature of 53°C. The early methanogenic source identified in B7a at about 28°C and a mixed source in B8 at about 36°C, could be the result of methane evolved from maturing hydrocarbons in lower horizons mixing with marine carbonate as suggested by Wood and Boles (1991). A more complex description of the pore fluid composition is possible, but is unlikely to change calculated temperatures by more than ± 15°C.

5.2. Thermal evolution of Elk Hills and extrapolation of temperature history to Stevens zone

The thermal history experienced by the Stevens sands at Elk Hills cannot be ascertained directly from K-feldspar $^{40}Ar/^{39}Ar$ studies due to the low temperatures experienced by these samples ($< \sim 95°C$). At these temperatures, no measurable loss of $^{40}Ar*$ from K-feldspar is expected. Nonetheless, knowledge of the general form of the depositional history together with K-feldspar $^{40}Ar/^{39}Ar$ results from greater depths permits extrapolation of thermal history to the level of the Stevens sands.

Detrital K-feldspars were obtained from arkosic sandstone cores at depths between 4.12 to 6.61 km. $^{40}Ar/^{39}Ar$ age spectra of these samples exhibit radiogenic ^{40}Ar loss that can clearly be ascribed to basin heating (Mahon et al., 1998). Use of the multidiffusion domain model (Lovera et al., 1989) permits thermal history information to be obtained from the $^{40}Ar/^{39}Ar$ data. The burial history, determined from basin stratigraphy, aided Mahon et al. (1998) in constructing a framework thermal history that was then refined by constraints derived from modeling the $^{40}Ar/^{39}Ar$ data. Once the thermal history had been determined for the lower horizons where the $^{40}Ar/^{39}Ar$ experiments were performed, the thermal history was then extrapolated to shallower intervals, appropriate for the Stevens zone, utilizing a conductive heat flow model (see Table 3). The temperatures of carbonate cementation, determined from calcite–H_2O oxygen stable isotope thermometry in the previous section, are then used to ascertain the timing of cementation.

The change in geothermal gradient with time inferred from the above calculations for the lower horizons bear on the magnitude of the geotherm at the time the Stevens sands were deposited. Using an average geothermal gradient value of 40°C/km for EH-3G-B-7 (B7) and the Elk Hills subsidence rate over the past 7 Ma, Mahon et al. (1998) predicted a temperature of 95°C at a depth of 2 km. This value is essentially identical to the estimated equilibrium formation temperature (Mark Wilson, pers. comm., 1996).

5.3. Timing and source of cementation in Stevens zone

Temperature histories estimated from thermochronometry for the Stevens sandstone over the

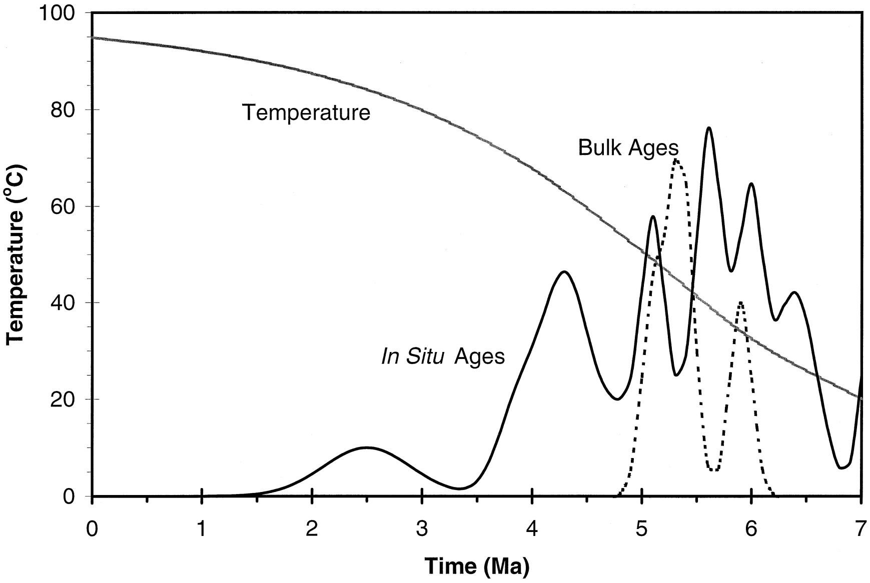

Fig. 5. The thermal history of the Stevens sands at a depth of 2200 m in well 352X-3G [see Part 1 of the work of Mahon et al. (1998)] with overlays of weighted histograms of calculated calcite precipitation age from in situ (solid line, 15 measurements) and bulk (dashed line, four measurements) oxygen isotope analyses. The temperatures of calcite precipitation are calculated by assuming a constant pore fluid composition equivalent to SMOW and the oxygen isotopic fractionation parameters for calcite–H_2O described by Friedman and O'Neil (1977). The derived temperatures are related to age of precipitation through the independently determined thermal history.

past 7 Ma (Table 3) and the calcite–H_2O oxygen stable isotope thermometry results (Table 4) permit model estimates of the timing of cementation. Fig. 5 is a plot of the calculated age of calcite precipitation vs. cumulative frequency. Note that nearly all the computed ages are 4 Ma or older, and that the bulk of the values are between 5 and 6.5 Ma. As expected for multiple generations of cementation, in situ isotopic measurements yield a greater spread than the data acquired by conventional means.

This data set indicates that cementation occurred early in the history of the reservoir and that the majority occurred over a relatively brief interval between 4 and 6.5 Ma. Combining textural relations with the in situ isotopic data provides a check on the model. The textural relations and microanalyses are consistent in that higher calculated precipitation temperatures correlate with textures indicative of later events. For example, B7a contains a cement precipitated at a model age of 6.4 Ma which is cross-cut by a calcite vein with a model age of 6 Ma. Much later generations of cement grow at 5.1 Ma and 4.3 Ma. Note that the bulk oxygen isotope value would indicate a single cementation event at 5.5 Ma.

The carbon isotope measurements give clues regarding the source of the fluid from which the cements were derived (Table 5). Carbon isotope analyses were in general performed close (within ~ 50 μm) to spots that had been analyzed for oxygen isotopes. In the B7a sample, the early cement was derived from a fluid containing light carbon ($\delta^{13}C_{PDB} = -9.0‰$). This may indicate an influence on the migrating fluid's composition from maturing hydrocarbons at far greater depths. The vein that cross-cuts this cement is likely to have evolved from a marine carbonate ($\delta^{13}C_{PDB} = +0.3‰$). The later cements appear to be from a mixed source ($\delta^{13}C_{PDB} = -7.3‰$). None of the measurements on this section resulted in an extremely light carbon isotopic signal characteristic of hydrocarbons ($\delta^{13}C_{PDB} < -20‰$; Emery and Robinson, 1993). This suggests that relatively little liquid hydrocarbon was present in the reservoir at the time of cementation of B7a, and thus the petroleum currently being extracted from this unit must have been introduced subsequent to 4.3 Ma (the time at which temperatures > 60°C were reached). Since the porosity was diminishing significantly following that time, we infer that the introduction of light carbon would have been from fluids derived locally, i.e., from the interbedded, organic-rich shales of the Monterey formation. Thus we would expect a relatively late maturation (the rocks have only now reached ~ 95°C) postdating the generally low temperatures recorded in the cements (Table 5).

Table 5
Model cementation temperature and carbon isotope composition

Sample	T (°C)	$\delta^{13}C_{PDB}$	Possible source
EH-3G-B-7a (B7a)			
bulk	42 ± 1	−4.3 ± 0.1%	Marine carbonate
in situ			
Cement-EH95	28 ± 4	−9.0 ± 0.5%	Methanogenic
Vein-EH95	33 ± 1	+0.3 ± 0.3%	Marine carbonate
Cement-EH96a	49 ± 2	−7.3 ± 0.6%	Mixed source
Cement-EH96a	62 ± 3	N/A	
EH-3G-B-8 (B8)			
bulk	35 ± 1	+1.9 ± 0.1%	Marine carbonate
in situ			
Cement-EH95	36 ± 5	−5.8 ± 0.5%	Mixed source
Cement-EH95	53 ± 6	N/A	
Calcite xtal-EH96a	28 ± 2	+6.2 ± 0.7%	Bacterial
Cement-EH96a	19 ± 1	N/A	
Cement-EH96a	41 ± 2	−0.7 ± 0.8%	Marine carbonate

Core B8 (EH-3G-B-8) experienced a similar diagenetic history to that of B7a. An early cement formed shortly after deposition at 7 Ma and was followed at about 6.4 Ma by the formation of subhedral crystals of calcite that can be identified in thin section. These crystals have a distinctive heavy carbon value of $\delta^{13}C_{PDB} = +6.2‰$. Wood and Boles (1991) interpreted the heavy carbon signal at NCL to be the result of bacterial influence that may have been present shortly after deposition. Calcite from a mixed source ($\delta^{13}C_{PDB} = -5.8‰$) precipitated at an estimated 5.8 Ma and was followed by a distinctively marine carbonate derived cement ($\delta^{13}C_{PDB} = -0.7‰$) at 5.6 Ma. Another generation of cement was identified to have precipitated at 4.8 Ma, but no reliable carbon measurements were made on this section.

Fig. 6 shows the relationship between the measured $\delta^{13}C_{PDB}$ and the estimated age of calcite cement precipitation obtained from both the in situ and bulk results. Although only three data points were

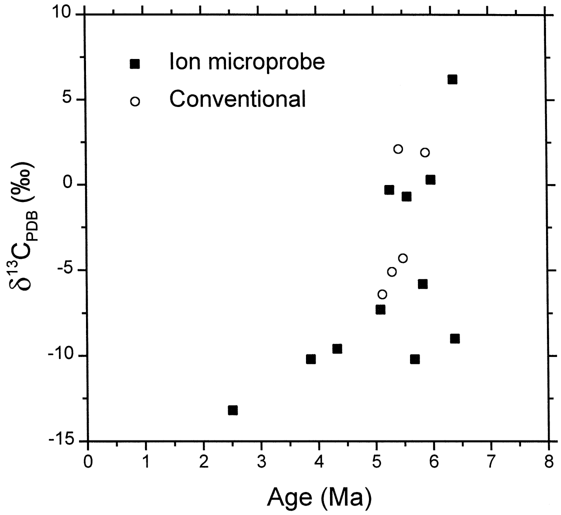

Fig. 6. Estimated cementation sequence at Elk Hills showing $\delta^{13}C$ vs. age of calcite precipitation. Bulk conventional analyses indicate a narrower range of both age and fluid composition than do the in situ analyses (see text for discussion).

obtained from cements with calculated ages < 5 Ma, they all contain isotopically light carbon consistent with a methanogenic source. Wood and Boles (1991) do not find such a late, isotopically light phase of calcite cementation. This may indicate a younger phase of maturation of the hydrocarbon at Elk Hills or perhaps reflect a limitation of bulk analysis.

Since the Stevens sands appear to have been largely cemented, and thus relatively impermeable, by ~5 Ma (Fig. 5), we conclude that the source of the of petroleum was likely from interbedded shales. However, since our temperature history calculations suggest that the oil generation window (80–100°C; Hunt, 1979) was not reached at depths appropriate to the Stevens sands until ~1–2 Ma, it follows that the liquid hydrocarbons extracted from the Elk Hills oil field are late Pliocene to Pleistocene in age.

The source of the migrating fluids responsible for precipitation of the cements is suggested by the carbon isotopic composition. Most of the fluids are of either a marine carbonate source or a mixture of marine carbonate and lighter carbon from maturing hydrocarbons. There are a few notable exceptions; one being subhedral crystalline material that appears to have been influenced by bacterial action and some cement that has a stronger influence from maturing hydrocarbons. A lighter hydrocarbon source provides carbon for the limited carbonate precipitation found after 5 Ma. Wood and Boles (1991) concluded that most of the cementation at NCL occurred between 4 to 5 Ma whereas our results are more consistent with a continuum of cementation. The later stages of carbonate cementation observed in the Wood and Boles study indicate a late phase of calcite precipitation from a marine source, whereas the latest phase of calcite precipitation revealed from in situ analysis at Elk Hills is from a fluid source with isotopically light carbon (see Fig. 6).

6. Summary and conclusions

The timing of carbonate cementation within the Stevens sands from Elk Hills was estimated using the thermal history developed by Mahon et al. (1998) and model precipitation temperatures based on in situ oxygen isotope analyses. The $^{40}Ar/^{39}Ar$ thermochronology results combined with available constraints on the subsidence history support a broadly linear heating during burial until approximately 6 to 9 Ma when there was a significant increase in heating rate. The Stevens sands, the focus of this study, were deposited at approximately 7 Ma (Wood and Boles, 1991; Calloway, 1990). Based on results from conductive heat flow models, the Stevens experienced the enhanced rate of temperature increase shortly after deposition.

Oxygen and carbon isotopic ratios were determined by ion microprobe in calcite cements from the Stevens sands. Model temperatures (calculated from oxygen isotope compositions using the calcite–H_2O thermometer) suggest that the majority of the calcite cement analyzed from the Stevens sands precipitated in a semi-continuous fashion after deposition at 7 Ma until about 3 Ma. These in situ measurements reveal a broader interval of cementation than bulk results and provide evidence of temporal variability in the carbon isotope composition of the source material. Sources of carbon responsible for these cementation events appear to be mostly of marine carbonate origin (with a possible early bacterial influence) and a later mixed methanogenic–marine carbonate source. Because bulk analyses average a continuous distribution, these results tend to provide information over a more limited time interval than the in situ measurements. The calcite cements inferred to have precipitated most recently (and thus at the highest temperatures) contain a light carbon signal, likely due to thermal decomposition of kerogen in the interbedded shales of the Stevens zone.

Acknowledgements

We thank the Department of Energy, Bechtel Petroleum Operations (BPOI), and the Chevron staff at NPR-1 for providing us with core materials and for their gracious assistance. In particular, we wish to acknowledge Mr. Dan Hogan (DoE) for providing access to the NPR-1 samples. We thank William Bartling (Chevron), Mark Wilson (BPOI), and George McJanet (DoE) for sharing their extensive experience of the Elk Hills oil field with us. We are grateful to Jim Sample for providing the Joplin calcite and unpublished isotopic results, and Ian Kaplan for suggesting Elk Hills as the test environment for studying isotopic variations in carbonate cements and undertaking carbonate isotopic analyses on our behalf. We thank Jim Boles for generously providing samples from North Coles Levee. Constructive criticism of the manuscript was received from David Awwiller, Jim Boles, Marty Grove, Rick Hervig, and John Valley, for which we are grateful. The UCLA ion microprobe laboratory is partially supported by a grant from the National Science Foundation Instrumentation and Facilities program.

Appendix A. Sample descriptions

A.1. Sample Series EH-3G-B

Calcite cemented arkosic sandstone from the upper Main Body B in the Stevens sands were obtained from well 352X-3G. Four 1-in. plugs were drilled from core obtained between depths of 2216.23–2217.08 m and are collectively referred to as EH-3G-B-6 (B6). Five 1-in. plugs from core obtained between depths of 2204.47–2204.59 m are collectively referred to as EH-3G-B-7 (B7). A single 1-in. plug from a depth of 2182.5 m is referred to as EH-3G-B-8 (B8). All three core intervals are calcite cemented. Cements occupy ~25% of the total rock volume and no quartz overgrowths were identified. These rocks are poorly sorted with detrital grains ranging in size from 2 mm–10 μm. Quartz predominates with subequal amounts of K-feldspar and altered plagioclase totalling ~30%. Lesser amounts (< 20%) of lithic fragments and micas are present. All rocks appear matrix supported indicating the introduction of the calcite cement before the sediment was fully compacted.

A.2. Sample Series NCL-29-A

Two cores from Stevens sands in North Coles Levee well 488-29 were obtained: NCL-29-A-1 (NCL1) was sampled at a drill depth of 2746.4 m and NCL-29-A-2 (NCL2) from 2727.4 m. Both samples are arkosic with subequal amounts of quartz and feldspar and the vast majority of detrital grains are between 0.1–1 mm in size. The proportion of cement in the NCL cores was smaller than that in the Elk Hills samples and a smaller proportion of the cement was calcite.

References

Bent, J.V.B., 1988. Paleotectonics and provenance of Tertiary sandstones of the San Joaquin basin, California. Studies of the Geology of the San Joaquin Basin. SEPM, Los Angeles, CA, pp. 109–120.

Boles, J.R., Ramseyer, K., 1987. Diagenetic carbonate in Miocene sandstone reservoir, San Joaquin basin, California. AAPG Bull. 70, 1475–1487.

Calloway, D.C., 1990. Organization of stratigraphic nomenclature for the San Joaquin basin, California. Structure, Stratigraphy and Hydrocarbon Occurrences of the San Joaquin Basin, California. SEPM and AAPG, Bakersfield, CA, pp. 5–22.

Craft, B.C., Hawkins, M., 1991. Applied Petroleum Reservoir Engineering, 2nd edn., revised by R.E. Terry. Prentice-Hall, Englewood Cliffs, NJ, 431 pp.

Craig, H., 1957. Isotopic standards for carbon and oxygen correction factors for mass-spectrometric analysis of carbon dioxide. Geochim. Cosmochim. Acta 12, 133–149.

Davis, T.L., Lagoe, M.B., 1988. A structural interpretation of major tectonic events affecting the western and southern margins of the San Joaquin Valley, California. Studies of the Geology of the San Joaquin Basin. SEPM, Los Angeles, CA, 351 pp.

de Chambost, E., Hillion, F., Rasser, B., Migeon, H.N., 1991. The

CAMECA ims 1270: a description of the secondary ion optical system. In: Benninghoven, H. et al. (Eds.), SIMS VIII Proceedings. Wiley, New York, pp. 207–210.

Ehrenberg, N., 1989. Assessing relative importance of compaction processes and cementation to reduction of porosity in sandstones: discussion; compaction and porosity evolution of Pliocene sandstones, Ventura Basin, California: discussion. AAPG Bull. 73, 1274–1276.

Emery, D., Robinson, A., 1993. Inorganic Geochemistry: Applications to Petroleum Geology. Blackwell, Oxford, 254 pp.

Feldman, M.D., Kwon, S.T., Boles, J.R., Tilton, G.R., 1993. Diagenetic mass transport in the southern San Joaquin basin, California, U.S.A.: implications from the strontium isotopic composition of modern pore fluids. Chem. Geol. (Isotope Geosci. Sec.) 110, 329–343.

Fishburn, M.D., 1990. Results of deep drilling: Elk Hills field, Kern County, California. Structure, Stratigraphy and Hydrocarbon Occurrences of the San Joaquin Basin, California. SEPM and AAPG, Bakersfield, CA, pp. 157–168.

Friedman, I., O'Neil, J.R., 1977. Compilation of stable isotope fractionation factors of geochemical interest. In: Fleischer, J.M. (Ed.), Data of Geochemistry, 6th edn. USGS Prof. Paper 440-KK, 12 pp.

Graham, C., Valley, J.W., 1996. Ion microprobe analysis of $^{18}O/^{16}O$ in authigenic and detritalquartz in the St. Peter Sandstone, Michigan Basin and Wisconsin Arch, USA; contrasting diagenetic histories. Geochim. Cosmochim. Acta 60, 5101–5116.

Graham, S.A., Williams, L.A., 1985. Tectonic, depositional and diagenetic history of Monterey Formation, central San Joaquin basin, California. AAPG Bull. 69, 385–411.

Hervig, R.L., Williams, L.B., Kirkland, I.K., Longstaffe, F.J., 1995. Oxygen isotope microanalyses of diagenetic quartz: possible low temperature occlusion of pores. Geochim. Cosmochim. Acta 59, 2537–2543.

Houseknecht, D.W., 1987. Assessing the relative importance of compaction processes and cementation to reduction of porosity in sandstones. AAPG Bull. 71, 633–642.

Hunt, J.M., 1979. Petroleum Geochemistry and Geology. Freeman, San Francisco, CA, 617 pp.

Ireland, T., 1995. Ion microprobe mass spectrometry: techniques and applications in cosmochemistry, geochemistry, and geochronology. Advances in Analytical Geochemistry 2, 1–118.

Killingley, J.S., 1983. Effects of diagenetic recrystallization on $^{18}O/^{16}O$ values of deep sea sediments. Nature 301, 594–596.

Kharaka, Y.K., Berry, F.A.F., Friedman, I., 1973. Isotopic composition of oil field brines from Kettleman North Dome, California and their geologic implications. Geochim. Cosmochim. Acta 37, 1899–1908.

Lovera, O.M., Richter, F.M., Harrison, T.M., 1989. $^{40}Ar^{39}Ar$ geothermometry for slowly cooled samples having a distribution of diffusion domain sizes. J. Geophys. Res. 94, 17917–17935.

Mahon, K.I., Harrison, T.M., Grove, M., 1998. The thermal and cementation histories of a sandstone petroleum reservoir, Elk Hills, California, Part I. $^{40}Ar^{39}Ar$ thermal history results. Geochim. Cosmochim. Acta 152, 227–256.

McJanet, G.S., 1993. Overview of geology, production and reservoirs at Elk Hills. AAPG Bull. 77, 708.

Nilsen, T.H., Sylvester, A.G., 1995. Strike-slip basins. In: Busbyand, C.J., Ingersoll, R.V. (Eds.), Tectonics of Sedimentary Basins. Blackwell, Cambridge, MA, 579 pp.

Pate, C.R., 1989. Assessing the importance of compaction processes and cementation to reduction of porosity in sandstones: discussion. AAPG Bull. 73, 1270–1273.

Reid, S.A., 1990. Trapping characteristics of upper Miocene turbidite deposits, Elk Hills field, Kern County, California. Structure, Stratigraphy and Hydrocarbon Occurrences of the San Joaquin Basin, California. SEPM and AAPG, Bakersfield, CA, pp. 141–156.

Richter, F.M., DePaolo, D.J., 1987. Numerical models for diagenesis and the Neogene Sr isotopic evolution of seawater from DSDP site 590B. Earth Planet. Sci. Lett. 83, 27–38.

Robinson, A.G., Coleman, M.L., Gluyas, J.G., 1993. The age of illite cement growth, Village Fields Area, southern North Sea: evidence from K–Ar ages and $^{18}O/^{16}O$ ratios. AAPG Bull. 77, 68–80.

Schrag, D.P., DePaolo, D.J., Richter, F.M., 1992. Oxygen isotope exchange in a two-layer model of oceanic crust. Earth Planet. Sci. Lett. 111, 305–317.

Schrag, D.P., DePaolo, D.J., Richter, F.M., 1995. Reconstructing past sea surface temperatures: correcting for diagenesis of bulk marine carbonate. Geochim. Cosmochim. Acta 59, 2265–2278.

Schultz, J.L., Boles, J.R., Tilton, G.R., 1989. Tracking calcium in the San Joaquin basin, California: a strontium isotopic study of carbonate cements at North Coles Levee. Geochim. Cosmochim. Acta 53, 1991–1999.

Slodzian, G., Chainteau, M.P., Dennebouy, R.C., 1987. SIMS: Self-regulated potential at insulating surfaces in presence of strong electrostatic field. CAMECA News, May 1987, pp. 1–6.

Taylor, T.R., Soule, C.H., 1993. Reservoir characterization and diagenesis of the Oligocene 64-Zone sandstone, North Belridge field, Kern County, California. AAPG Bull. 77, 1549–1566.

Tieh, T.T., Berg, R.R., Popp, R.K., Brasher, J.E., Pike, J.D., 1986. Deposition and diagenesis of upper Miocene arkoses, Yowlumne and Rio Viejo fields, Kern County, California. AAPG Bull. 70, 953–969.

Valley, J.W., Eiler, J.M., Graham, C.M., Gibson, E.K., Romanek, C.S., Stolper, E.M., 1997. Low-temperature carbonate concretions in the Martian meteorite ALH84001: evidence from stable isotopes and mineralogy. Science 275, 1633–1638.

Wood, J.R., Boles, J.R., 1991. Evidence for episodic cementation and diagenetic recording of seismic pumping events, North Coles Levee, California, U.S.A. Appl. Geochem. 6, 509–521.

Woodruff, R., Savin, S.M., Douglass, R.E., 1981. Miocene stable isotope record: a detailed deep Pacific Ocean study and its paleoclimatic implications. Science 212, 665–668.